

Open  
Access

# Computational and Experimental Investigations of the Impacts of Window Parameters on Indoor Natural Ventilation in “Sultan Al-Ashraf Qaytbay” Mosque

Amr Gomaa Mohammed<sup>1,\*</sup>, Ahmed Farouk Abdel Gawad<sup>2</sup>, Mofreh Melad Nassief<sup>2</sup>

<sup>1</sup> Department of Mechanical Engineering, Higher Technological Institute, Egypt

<sup>2</sup> Department of Mechanical Power Engineering, Faculty of Engineering, Zagazig University, Egypt

## ARTICLE INFO

### Article history:

Received 15 November 2019

Received in revised form 10 January 2020

Accepted 26 January 2020

Available online 13 April 2020

## ABSTRACT

Sultan Al-Ashraf Qaytbay mosque is viewed as one of the most beautiful achieved landmarks of late Egyptian Mamluk architecture. The mosque architectural design is considered exceptional for its refined extents and the subdued yet exquisite decorations. In this paper, Computational fluid dynamics (CFD) simulation joined with wind tunnel experiments are performed to investigate the airflow characteristics inside the mosque of Sultan Al-Ashraf Qaytbay due to natural ventilation brought about by window openings. Wind tunnel experiments are performed to provide the boundary conditions for the subsequent CFD simulations. The results of CFD simulation are contrasted with that of the wind tunnel experiments. The comparison demonstrates great agreement between the computational and experimental results, which confirms the legitimacy of the present computational procedure. Interesting outcomes and productive conclusions are inferred from the obtained results.

### Keywords:

Archaeological mosque; natural ventilation; computational fluid dynamics (CFD); wind tunnel experiments

Copyright © 2020 PENERBIT AKADEMIA BARU - All rights reserved

## 1. Introduction

Ventilation is the air exchange between inside and outside conditions of a structure by means of the wind flow which is viewed as a principal necessity to the building occupancy [1]. In moderate climates, common ventilation, in the present-day structures, is generally organized by open windows rather than specialized design elements. Appropriately, the position of window openings is viewed as a significant parameter deciding the adequacy of wind-driven cross-ventilation in buildings.

\* Corresponding author.

E-mail address: [amro.gomaa.hti@gmail.com](mailto:amro.gomaa.hti@gmail.com) (Amr Gomaa Mohammed)

<https://doi.org/10.37934/arfmts.69.2.1941>

Consequently, natural ventilation can spare the energy devoured by the heating, ventilating, and air-conditioning (HVAC) systems in the event that it provides adequate indoor air quality and thermal comfort levels.

### 1.1 Present Case Study

Sultan Al-Ashraf Qaytbay mosque, as appeared in Figure 1, is an archaeological mosque worked by Sultan Al-Ashraf Qaytbay in Cairo's Northern Cemetery, which is situated on Muizz Street. The Sultan Al-Ashraf started its construction in 826 AH/1424 AD and finished in 1474 AD [2-3]. The mosque is characterized by the excellence of its structural plan so that it was pictured on the Egyptian one-pound note.



**Fig. 1.** A photographic view of Sultan Al-Ashraf Qaytbay mosque

The mosque's entrance faces north and occupies the fundamental street somewhat eastwards around the walls of the tomb, perhaps to upgrade its special visualization. Figure 2 demonstrates a schematic outline of the Sultan Al-Ashraf Qaytbay mosque internal space.

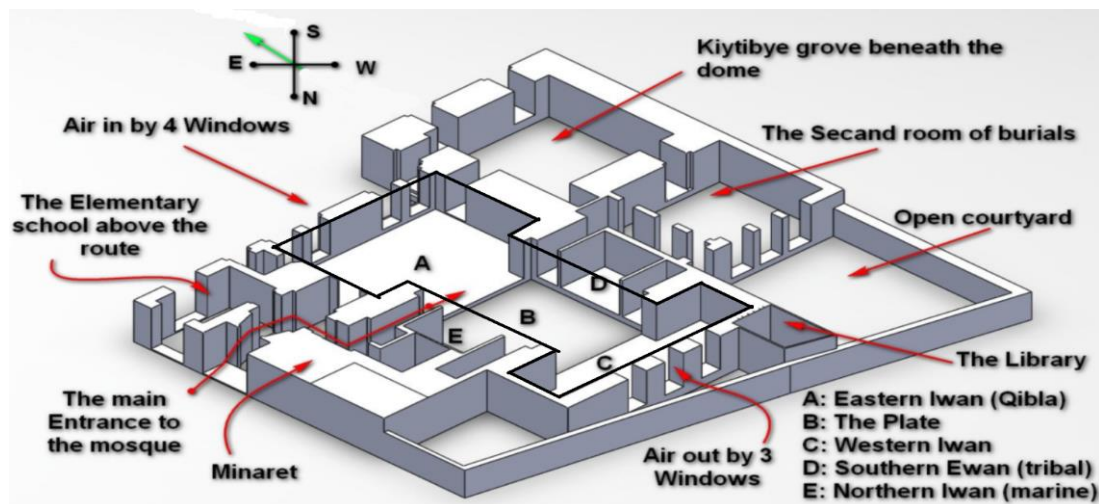


Fig. 2. Schematic diagram of the Sultan Al-Ashraf Qaytbay mosque internal space

## 1.2 Previous Investigations

### 1.2.1 CFD-based simulations

In the previous decade, numerous advances have been made in different uses of CFD in natural ventilation researches. In this manner, CFD-based simulations have turned out to be one of the most valuable instruments for in-depth investigations of building architectural design and wind conditions in recent years.

In this context, Allocca *et al.*, [4] developed a CFD model to concentrate on single-sided normal ventilation so as to decide the influence of the wind flow on the ventilation rates and indoor conditions. The outcomes demonstrated that wind flow has numerous favourable circumstances, including an agreeable and healthy indoor condition and sparing energy by methods of passive cooling or natural ventilation. Likewise, an examination utilizing Fluent CFD programming was directed by Song and Meng [5] to improve ventilation execution in a study hall. In light of the simulation data, it is discovered that double rows windows can improve the thermal comfort conditions most effectively, thus exhaust fans and ceiling fans, however, ceiling fans could improve the environment of occupied zones better. Wang *et al.*, [6] examined single-sided regular ventilation driven by buoyancy and wind through variable windows utilizing CFD. Their outcomes uncovered that the ventilation rate commonly expanded with increasing wind speed. Additionally, Deng *et al.*, [7] enquired numerically and experimentally the local thermal comfort in an open-plan office with an automatic controlled natural ventilation system. A computational fluid dynamics (CFD)-established method was exhibited for indoor environment. Long-term in-situ measurement was conducted during summer and transition seasons. The numerical results unveiled an adventure of local thermal dissatisfaction below low outdoor temperature and strong windy conditions.

### 1.2.2 General indoor natural ventilation

As well, the verification of the original building design and the effect of windows and balconies on natural ventilation had to be counted in assorted studies. From these analyses, Wu *et al.*, [8] accounted for a computational framework to assert the original design concept in the layout of natural ventilation for the Tjibaou Cultural Center. Simulated results were bespoke that the ameliorated design considerably enhanced the air-intake effectiveness and realized a satisfactory

pressure balance for the Tjibaou Cultural Center. ventilation on buildings. The window opening configuration for thermal comfort in naturally ventilated buildings was elevated by Stavrakakis *et al.*, [9]. The airflow in and around the building is simulated employing a CFD model. It was concluded that the proposed methodology allowed the optimum window designs, which correspond to the dearest objective variables for both single and various activity levels. Mohamed *et al.*, [10] evoked that balconies could ameliorate the level of thermal comfort and indoor air quality of apartments for high-rise building by offering greater indoor air speed and better ventilation performance, respectively. The natural ventilation rate imputable the buoyancy effect for assorted types of windows and discovered large variances in ventilation rate was experimentally enquired by Grabe *et al.*, [11]. The obtained results evidenced the importance of considering divergent window types when calculating the ventilation rate.

Experimental and numerical investigations for evaluating the effects of natural ventilation on the thermal comfort within residential buildings was preceded by Elshafei *et al.*, [12]. Validation of the simulation outcomes was executed employing experimental measurements. Their outcomes reflected the demand for design alterations in window parameters (window sizing, window locating, and shades) to ameliorate the thermal comfort within the domain. Zhou *et al.*, [13] developed a model for predicting the total flow rate of single-sided natural ventilation motivated by the fact that the wind-driven ventilation itself is commonly considered to consist of two components; a mean component and a fluctuating component.

The developed model showed that the total flow rate is majorly caused by pulsating flow when the area of the opening was small, but it was mainly caused by mean flow in the case of a large opening. Also, Heracleous and Michael [14] investigated the indoor comfort conditions in a typical classroom of a secondary school in Cyprus and explore the effect of natural ventilation on both thermal comfort and air quality. For the aims of the analyse, indoor and outdoor environmental conditions were monitored. Versatile ventilation schemes and window opening patterns were utilized, in order to distinguish the best option to exploit natural ventilation as a way to attain optimum air quality, particularly during wintertime. the study demonstrated that selected ventilation patterns, and window opening patterns, admitted the melioration of air quality with minimum heat losses in wintertime.

### 1.2.3 Wind tunnel experiments

For concentrates on natural ventilation, wind tunnel experiments are a reliable tool for the determination of the impacts of wind loads on different structures in addition to the impact of natural ventilation on buildings, which is the particular purpose of this research. In wind tunnel experiments, wind flow with controlled speed and bearing flow over small models, to recreate the regular ventilation of the structures. Wong and Heryanto [15] utilized CFD simulation and wind tunnel experiments to study the capability of utilizing an active stack to upgrade regular ventilation in residential apartments in Singapore. The outcomes identified the real plan parameters that significantly impact ventilation execution. Wind tunnel experiments were led by Chu *et al.*, [16] to examine the wind-driven ventilation for structures with two openings on a single wall. The outcomes demonstrated that the ventilation rate can be anticipated by the opening condition and the conversion standard was relative to the root-mean-square of the pressure fluctuation Wang *et al.*, [17] exhibited an exploratory and numerical assessment of the effects of opening structures on ventilation rates. The predictions agreed with the measured outcomes inside an error of 25%, and the new models can be utilized for the structure of the characteristic ventilation system. Sacht *et al.*, [18] provided details regarding the results of wind tunnel experiments directed for the assessment

of the impact of the situating and sort of network of ventilation modules on a façade system. Their outcomes demonstrated that wind tunnel experiments are dependable instruments for the assurance of the impact of natural ventilation.

#### 1.2.4 Natural ventilation in mosques

Mosques differ from other types of buildings as they are used at different hours and intervals and by experiencing an intermittent operation schedule. Therefore, they should be analyzed differently from residential and office buildings in terms of thermal comfort.

Ghaleb *et al.*, [19] represented an analysis on thermal comfort in the Al-Jawahir Mosque, sited in Johor Bahru, Malaysia. The aims were to evaluate the thermal comfort interior of the mosque under the current ventilation system. Computational fluid dynamics (CFD) method was employed to accomplish flow simulations and the results were then compared to the limits stated in the ASHRAE Standard-55. Results of CFD simulations demonstrated that installing four exhaust fans preceding the windows on the west-side wall of the mosque was the most effective strategy to ameliorate the thermal comfort interior the mosque.

Bughrara *et al.*, [20] studied the potential of applying an underfloor heating system for melioration of indoor thermal comfort in a historical mosque, which was naturally ventilated, heated and cooled, based on adaptive thermal comfort technique. The chosen Salepçioğlu Mosque was constructed in 1905 in Kemeraltı, Izmir, Turkey. Dynamic simulation modelling tool, DesignBuilder v.4.2 was employed to create the physical model of the Mosque. The ASHRAE Guideline 14 indices were employed to calibrate the model. The results of calibrated baseline model showed that the Mosque does not fulfil satisfactory thermal comfort levels for winter months that furnished by the accommodative method. Also, Hussin *et al.*, [21] enquired the thermal comfort performance of large-scale retrofitted air-conditioned mosques with intermittent operation in Penang, Malaysia. The case study was conducted on a large-scale mosque with a floor area of 2,920 m<sup>2</sup> that is provided with a centralized air-conditioning system. Result demonstrated that the system acquired an indoor thermal environment that inside the range advocated by ASHRAE Standard 55. In addition, Atmaca and Gedik [22] analyzed the indoor thermal comfort levels in two mosques that had natural and mechanical ventilation systems, besides various heating-cooling systems. The thermal comfort values were compared to international standards. It was found according to the measurements that the zone closes to the mosque entrance area had the lowest thermal comfort level. The thermal comfort level of the mosque entrance regions should be ameliorated by employing architectural elements (windbox, etc.) or mechanical equipment (air curtain, etc.).

#### 1.2.5 Important and significance of the present study

Based on the above illustrations of previous researches of other investigators the following points represent a strong motivation to the present work and highlight its innovative significance:

- i. Most of the researches concentrate on modern buildings. Very few consider the natural ventilation of ancient buildings such as mosques.
- ii. Even the researches that consider mosques are mainly directed to modern ones that were constructed in the twelfth century with the application of modern ventilation concept and techniques.
- iii. Based on the author's experience, there is very limited consideration of the natural ventilation techniques that were applied in constructing the ancient mosques in Egypt, although most of these mosques are still performing worshipping services in daily bases.



- iv. The study of ancient techniques of natural ventilation is a vital issue in Egypt, as a developing country, considering the expected saving in energy and cost in comparison to the modern (artificial) ventilation techniques.
- v. The present study stands in a priority situation when considering the big number of ancient mosques, churches, and structures that exist in Egypt. Most of these structures were dating to hundreds of year ago. Furthermore, the overall climate conditions of the present time are very similar to those of hundreds of years ago.
- vi. Thus, the present study is a notable addition to the study of natural ventilation concepts of ancient structures in historical countries such as Egypt.

## 2. Methodology

In the present study, wind tunnel experiments are performed with a reduced scale model of the mosque to expand the reliability and viability of development, diminish costs, and empower the assessment of the impact of current mosque structure from the characteristic ventilation perspective. The wind tunnel experiments are completed in an open-circuit, blowing-type wind tunnel. A photograph of the wind tunnel is shown in Figure 3.



Fig. 3. Photo of the used wind tunnel

The tunnel is operated by a delivery axial-fan. The total length of the wind tunnel is 6.0 m and situated 1.0 m over the floor. The test segment is 0.6 m long with a square cross-section of 0.5 m × 0.5 m. The tunnel is furnished with different flow- conditioning gadgets before the entrance of the test section to accomplish the uniform flow with the minimum boundary layer. The specifications of the driving motor of the wind tunnel are listed in Table 1.

**Table 1**

Specifications of the axial-fan electric motor

Specification	Value
Type	ADM-180M-4 NO
Power	15 HP
Speed	1480 RPM
$\Delta / Y$	380 / 630
AMP	22.3 / 12
Frequency	60 HZ

## 2.2 Experimental Model

Precisely to represent airflow attributes inside the mosque through natural ventilation and to examine the thermal comfort and suitability of the place, where the praying rituals are held, a geometrical model is planned and built up. Taking note of that, the phenomena observed in both the model and the mosque must be equivalent if the principles of physics and conditions contour are similar.

The geometrical model utilized in this examination represents the principal part of the mosque where the praying happens. The overall dimensions of the mosque have been acquired from the Egyptian Ministry of Antiquities [23]. A field visit to the compound of Sultan Al-Ashraf Qaytbay is completed, where any extra measurements are taken legitimately from the site. The proportion of the model to the genuine mosque is 1:40. In this way, the general components of the model are: length = 512 mm, width = 325 mm, and height = 400 mm. The walls of the model are made from smooth straightforward acrylic plates of 4 mm thickness. The acrylic plates are cut by a laser cutting machine to the expected measurements to guarantee most extreme conceivable precision. AutoCAD 2018 is the product that is utilized to set up the drawings that are bolstered to the laser cutting machine in order to cut the walls that represent the model faces. After that, 840 holes with measurement 1.7 mm are bored into the model faces.

These holes are utilized to embed the pressure taps that are made of small copper capillary tubes with a length of 10 mm and 1.7 mm measurement. The copper taps are fixed into their places utilizing a reasonable adhesive paste. These tubes are associated with the Multi-manometer by rubber tubes (hoses) of 2 mm diameter. CAD assembly drawing of the model is shown in Figure 4.

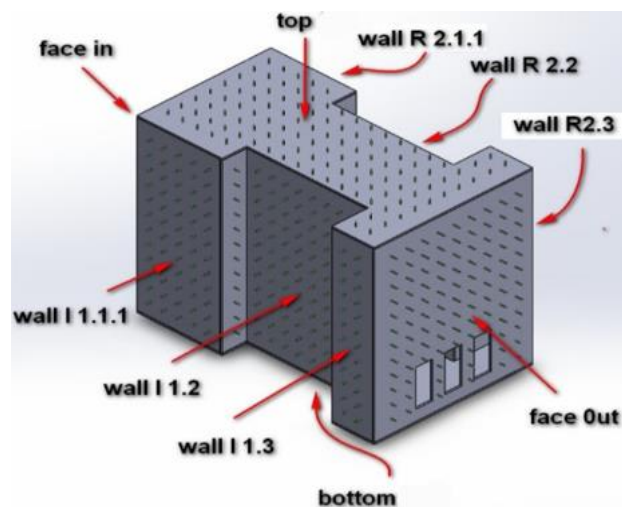


Fig. 4. A CAD drawing of the model

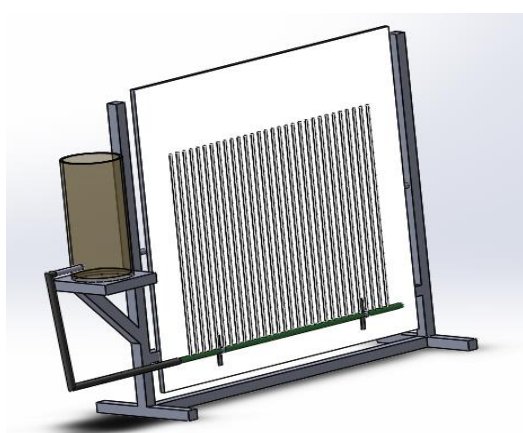
To guarantee precise estimations and anticipate the undesirable interference between the external wind flow and the copper taps, an external wall was added to the model. Therefore, the external components of the model are: length ( $l$ ) = 580 mm, width ( $w$ ) = 480 mm, and height ( $h$ ) = 480 mm. Cautious precautionary measures are taken to anticipate air leakage to the space between the internal and external walls of the model. final assembly of the acrylic model is shown in Figure 5. As it can be noticed in Figure 5 and Figure 6, the praying section has seven windows, four in the inlet face and three in the outlet face. The model dimensions of these windows are 35 mm-width ( $w$ ) and 85 mm-height ( $h$ ).



**Fig. 5.** Photo of the model with the outer walls

### 2.3 Measurements

In such examinations, it is essential to measure two variables, which are approaching the air speed flow of the model, and static pressure dissemination on the model walls. A multi-manometer is utilized to record the values of the static pressure. Because of the huge number of measuring points in the present examination, a multi-tube manometer was built and utilized, Figure 6(a). As found in Figure 6(b), the multi-manometer comprises of a metal holder of length 2.0 m, and height 1.5 m, and a wooden leading body of  $1.5 \times 1.5 \text{ m}^2$ . On the lower some portion of the wooden board, a 25 mm-distance across PVC pipe, drilled with 30 holes, represents to the feeder of the measuring liquid. One end of the feeder is closed while the opposite end is associated with a tank at a height of 50 cm over the feeder by a flexible hose. Thirty glass tubes with length 1.0 m and distance across 8 mm are fixed at their lower end to the PVC feeder through the penetrated holes utilizing adhesive paste. While the opposite end is associated with 30 flexible transparent hoses (tubes) with a width of 1.7 mm and length of 1 m. These adaptable tubes are associated with the pressure taps on the model walls.



(a)



(b)

**Fig. 6.** Multi-meter of the present study, (a) CAD drawing, (b) photographic view

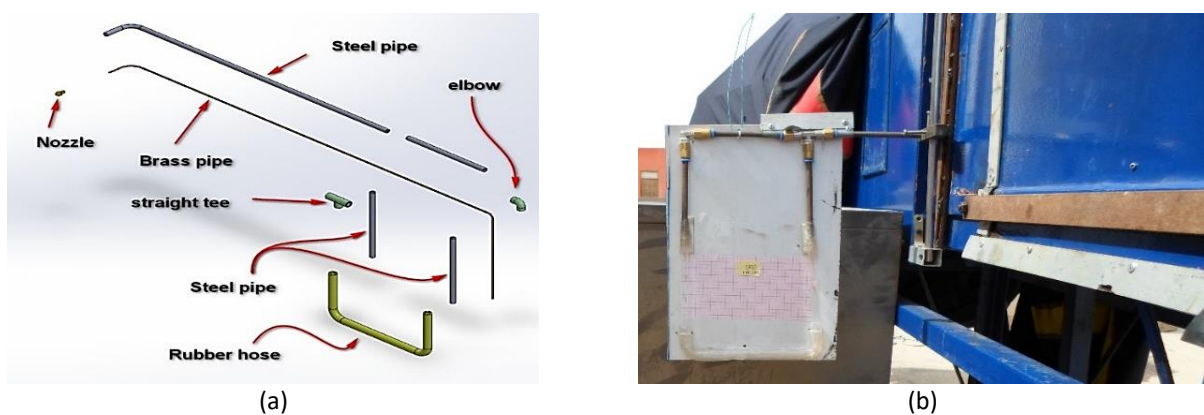
Speed is estimated utilizing a Pitot-static tube, while pressure taps are utilized to measure the static pressure difference. In the present investigation, a standard Pitot-tube was manufactured [24].



As appeared in Figure 7(a), the Pitot-tube was created from a metal capillary tube (inner tube) of length 900 mm and width 1.7 mm capsulated in a steel tube (external tube).

The steel tube comprises of two steel tubes of absolute length 550 mm, external width 8 mm, and an inward diameter of 5 mm. Likewise, two identical steel channels of length 150 mm, external measurement 8 mm, and an internal width of 5 mm are associated together utilizing straight T-and elbow-connections.

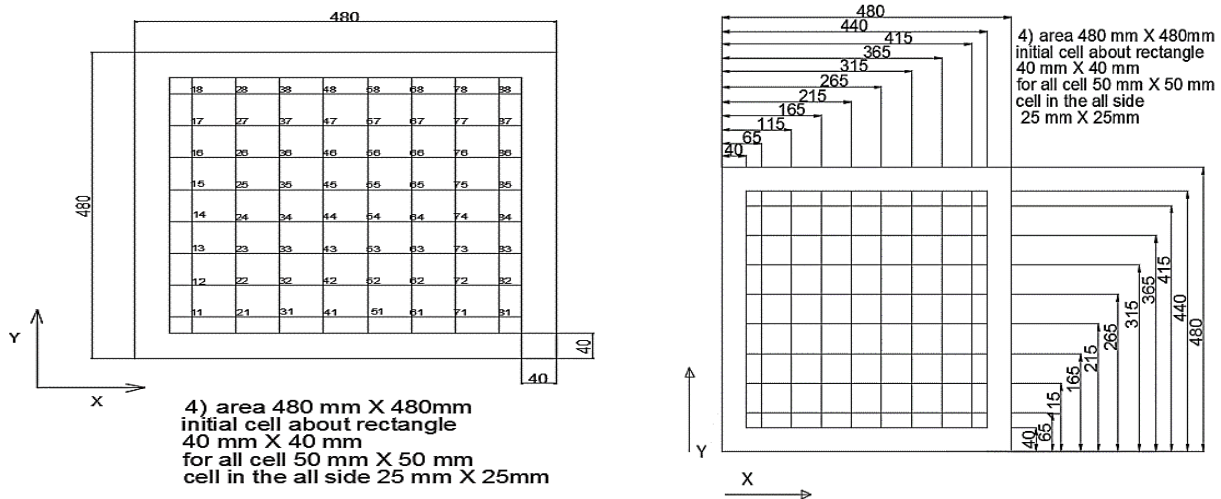
The lower parts of the two identical steel pipes are connected to flexible transparent hoses that are connected to the two terminals of the U-tube manometer, Figure 7(b). A nozzle of length 10 mm and external and internal diameter 8 mm, and 1.7 mm, respectively was fixed at the tip of a brass capillary tube (inner tube) to measure the total pressure. Three small openings of the distance across 1.0 mm were bored on the steel tube (external tube). The three holes are equally distributed along the circumference of the tube to measure static pressure. At last, the Pitot-tube and its U-tube manometer are fixed on 200 mm × 300 mm steel board.



**Fig. 7.** Pitot-tube of the present study, (a) Drawing of the components, (b) Pitot-tube fixed in place during experiments

To compute the velocity distribution of the approaching air flow towards the front mass of the model utilizing the Pitot-tube, the cross-sectional area of the wind tunnel, which is 480 mm × 480 mm with active zone 400 mm × 400 mm, was partitioned into rectangular/square grid cells. The border grid cells had dimensions of 50 mm × 25 mm, while the interior grid elements had dimensions of 50 mm × 50 mm.

The measuring points were situated at the intersections of the grid cells. Subsequently, the total number of measuring points was 64. The details of the frontal area with the grid cells are shown in Figure 8.



**Fig. 8.** The grid of the location of the measuring points

## 2.4 Estimation of Experimental Errors

The affectability of any device constrains its precision; the base division of an instrument implies the minimum accurate readable value. Aggregation of the errors associated with estimating or ascertaining the parameters will cause the deviation of the determined outcomes. The uncertainty in the calculated experimental results on the basis of the uncertainties in the primary measurements can be estimated by the method presented by Kline and McClintock [25]. To assess the uncertainty in the determined outcomes dependent on the uncertainties in primary measurements, the following formula is recommended.

$$\omega_R = \left[ \left( \frac{\partial R}{\partial X_1} \omega_1 \right)^2 + \left( \frac{\partial R}{\partial X_2} \omega_2 \right)^2 + \dots + \left( \frac{\partial R}{\partial X_n} \omega_n \right)^2 \right]^{0.5} \quad (1)$$

where,  $\omega_R$  is the uncertainty in the final result,  $X_1, X_2, \dots, X_n$  are the independent variables,  $\omega_1, \omega_2, \dots, \omega_n$  are the uncertainty in independent results,  $R$  is the function of the independent variables  $X_1, X_2, X_3, \dots, X_n$ . Then, the relative error  $\lambda_R$  (%) is defined as follows.

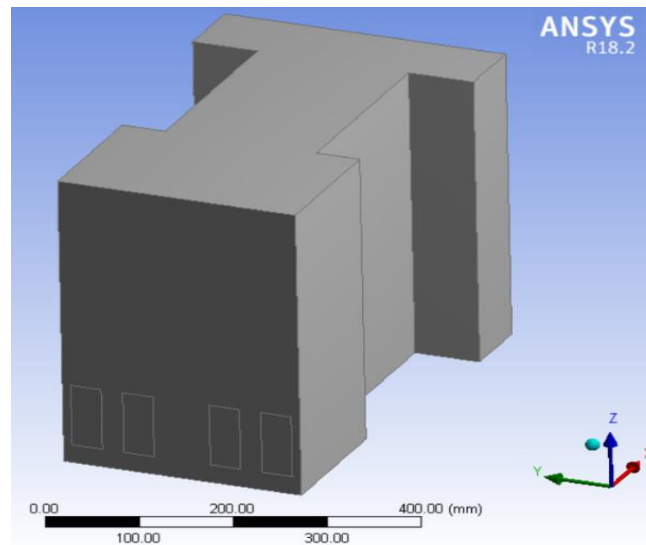
$$\lambda_R = \frac{\omega_R}{R} \times 100 \quad (2)$$

The relative error for each variable is calculated from the experimental data as follows, in pressure (P)  $\pm 8.33\%$ , in velocity (V)  $\pm 0.21\%$  and in the coefficient of pressure (Cp)  $\pm 0.0047\%$ .

## 3. Aspects of Computational Fluid Dynamics (CFD) Simulations

### 3.1 CFD Settings and Parameters

ANSYS Fluent [26] is the CFD software utilized for simulation in the present investigation. For all the explored cases, the wind speed is aimed at zero- incidence, perpendicular to the front wall of the mosque (in the horizontal x-heading). Five distinctive wind speeds were researched, in particular: 3, 5, 10, 15, and 20 m/s. The computational domain and corresponding axis-orientation are shown in Figure 9. Normally, the outside wind flow is fierce. Hence, Thus, the k- $\epsilon$  model is utilized as the turbulence model of the solution.

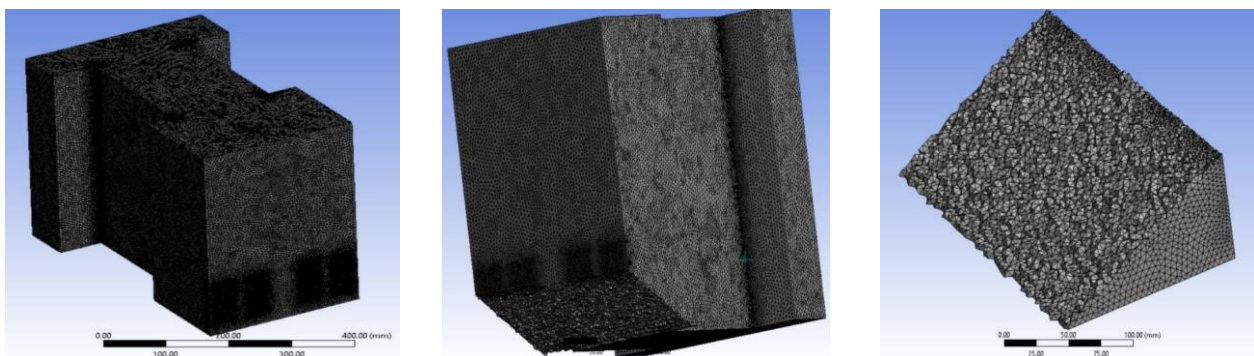


**Fig. 9.** Computational domain and corresponding axis-orientation

For the present CFD analysis, the 3D-model was created utilizing ANSYS Design Modeler [27]. As the study concerns the flow field inside the mosque, the computational model is similar to the experimental model for the sake of comparison and validation.

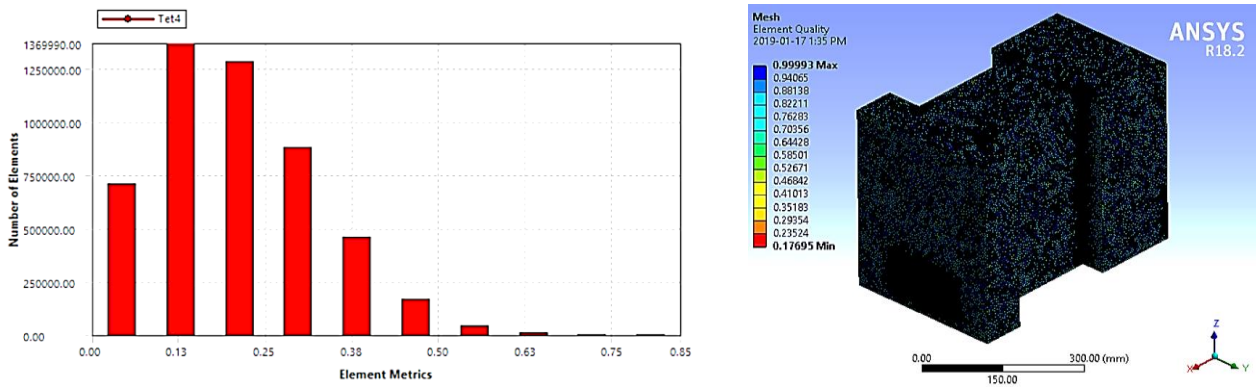
### 3.2 Meshing

Creating the most appropriate mesh is the foundation of CFD engineering simulations. In this way, the computational domain is discretized into 4,036,172 elements. To guarantee accurate outcomes, the size of elements at critical regions (windows openings and corners) were exceptionally decreased. The meshed 3D model is illustrated in Figure 10.



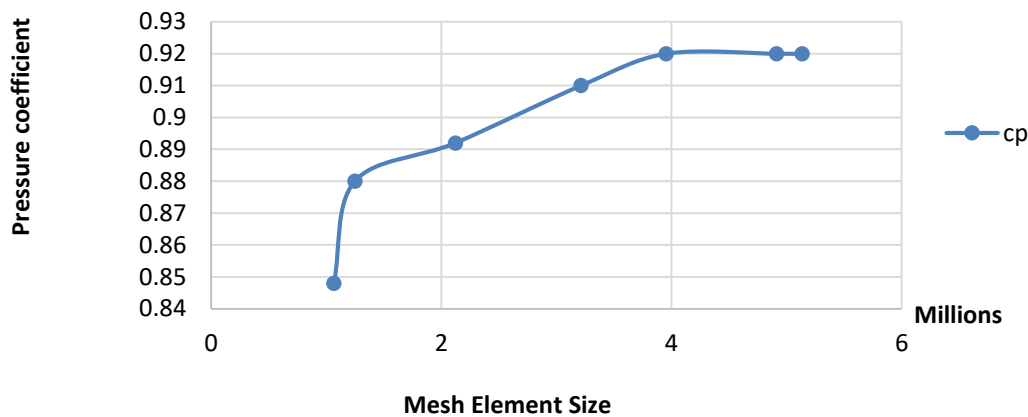
**Fig. 10.** Different views of the meshed 3D model

To guarantee the mesh-independency of the computational solution, diverse mesh sizes of 3125470, 3704508, 4036172, and 7835076 are considered as can be found in Figure 11. Note that the arrangement was almost constant starting from the mesh size of 4036172.



**Fig. 11.** Mesh-independency study for the simulated model

Figure 12 shows the variation of CP value, at certain location with the increase of the mesh size. It is clear from the figure that there is no remarkable variation of CP value behind the mesh size 4,917,336. Thus, the mesh size of 4,917,336 was chosen to carry out the computations to save computer run-time.

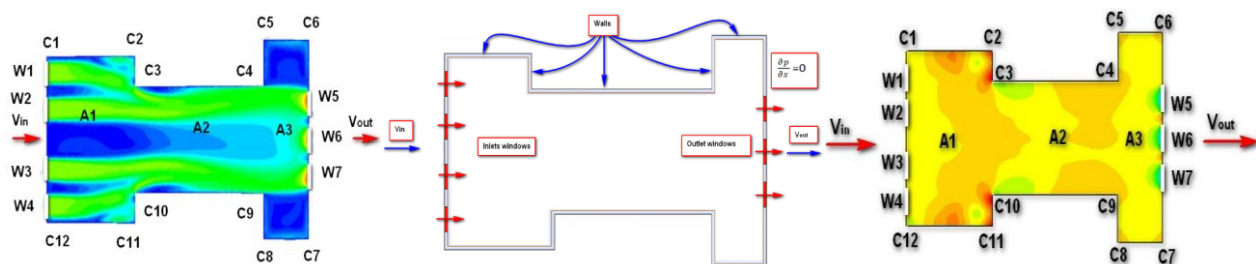


**Fig. 12.** Mesh independency

### 3.3 Boundary Conditions

As the airflow is incompressible, the flow density was assumed to be consistent with a value of 1.225 kg/m<sup>3</sup>. As shown in Figure 13 The velocity value is set at the inlet openings of the model (bay windows on the front wall) as the channel limit condition.

"Pressure outlet" is utilized as the outlet boundary condition at the outlet of the computational domain (outlet windows on the rear wall). All other faces of the model, including side walls, floor, and ceiling, are considered as smooth walls. Inlet turbulence intensity was set as 5%.



**Fig. 13.** Boundary conditions illustrations

**Table 2**  
 Values of flow characteristics

Flow characteristic	Value
$V_{in}$	3,5,10,15,20 m/s
$\rho$	1.225 kg/m <sup>3</sup>
T	25°C
Turbulence intensity	5%
Bounding Box	
Length X	512 mm
Length Y	325 mm
Length Z	400 mm
Properties	
Volume	4.806e+007 mm <sup>3</sup>
Centroid X	-45.462 mm
Centroid Y	$3.7599 \times 10^{-15}$ mm
Centroid Z	200 mm
Statistics	
Nodes	856,256
Elements	4,917,336

## 4. Results

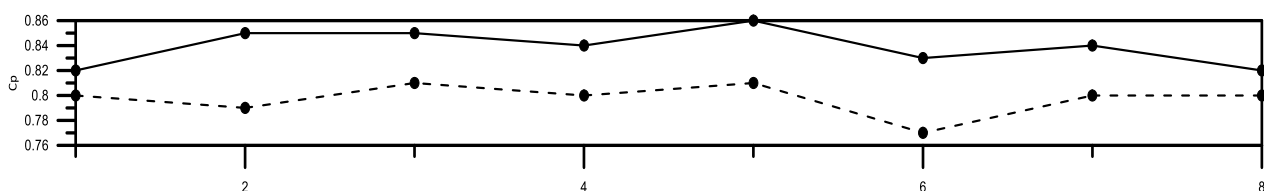
### 4.1 Pressure Distribution

In this segment, the experimental and CFD results are discussed and interrupted. Where, five flow speeds are simulated including 3, 5, 10, 15, and 20 m/s, because of confinements of the experimental facility and with the end goal of approval, the air velocity of the investigations was fixed at 20 m/s. Air speed and pressure differences over different walls of the model in addition to the flow flowlines are delineated and examined.

### 4.2 Comparison between CFD Simulations and Wind Tunnel Measurements

This is due to the limited space of the experimental model. Thus, the averaging of the computational results on each face is expected to be more accurate than the averaging of the experimental results on the same face as the measuring points do not cover the whole surface. Moreover, the effect of the measuring uncertainty, even its small magnitude, is expected to show up when compared with the computational results.

For more validation of the accuracy of the present computational model, Figure 14 shows a comparison between the computational and experimental results at a line above the ground by 0.8 m on the side wall. Generally, the comparison of the outcomes endorses confidence in the computational results. The maximum discrepancy is found to be 5%. Thus, the comparison of the outcomes endorsed the sensibility of the computational results.



**Fig. 14.** Comparison between present experimental and computational values of  $C_p$  at 20 m/s



### 4.3 Effect of Inlet Airflow Velocity

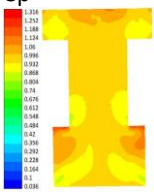
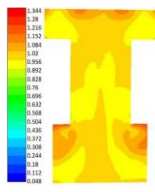
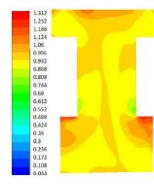
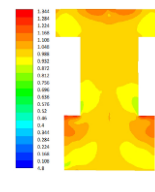
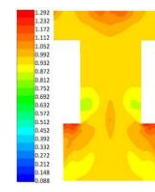
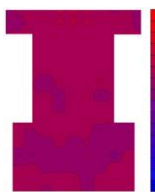
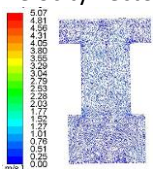
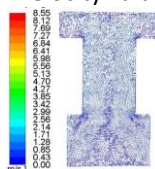
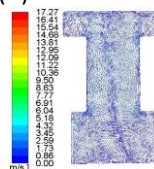
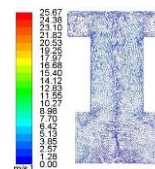
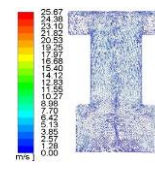

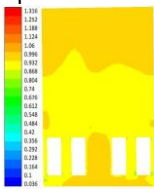
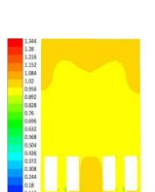
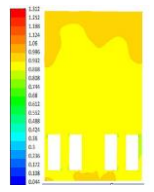
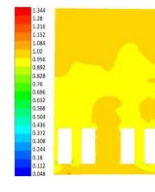
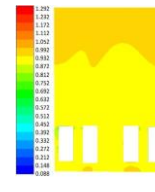

For all the explored cases, the distributions of  $C_p$  on all walls of the mosque model, alluding to Figure 9, are appeared in Table 3, which incorporates the distributions of the  $C_p$  just as well as velocity vectors for various inlet air velocities (3, 5, 10, 15, and 20 m/s). Likewise, the comparison with experimental results, at the available velocity of 20 m/s, is shown in Table 3.

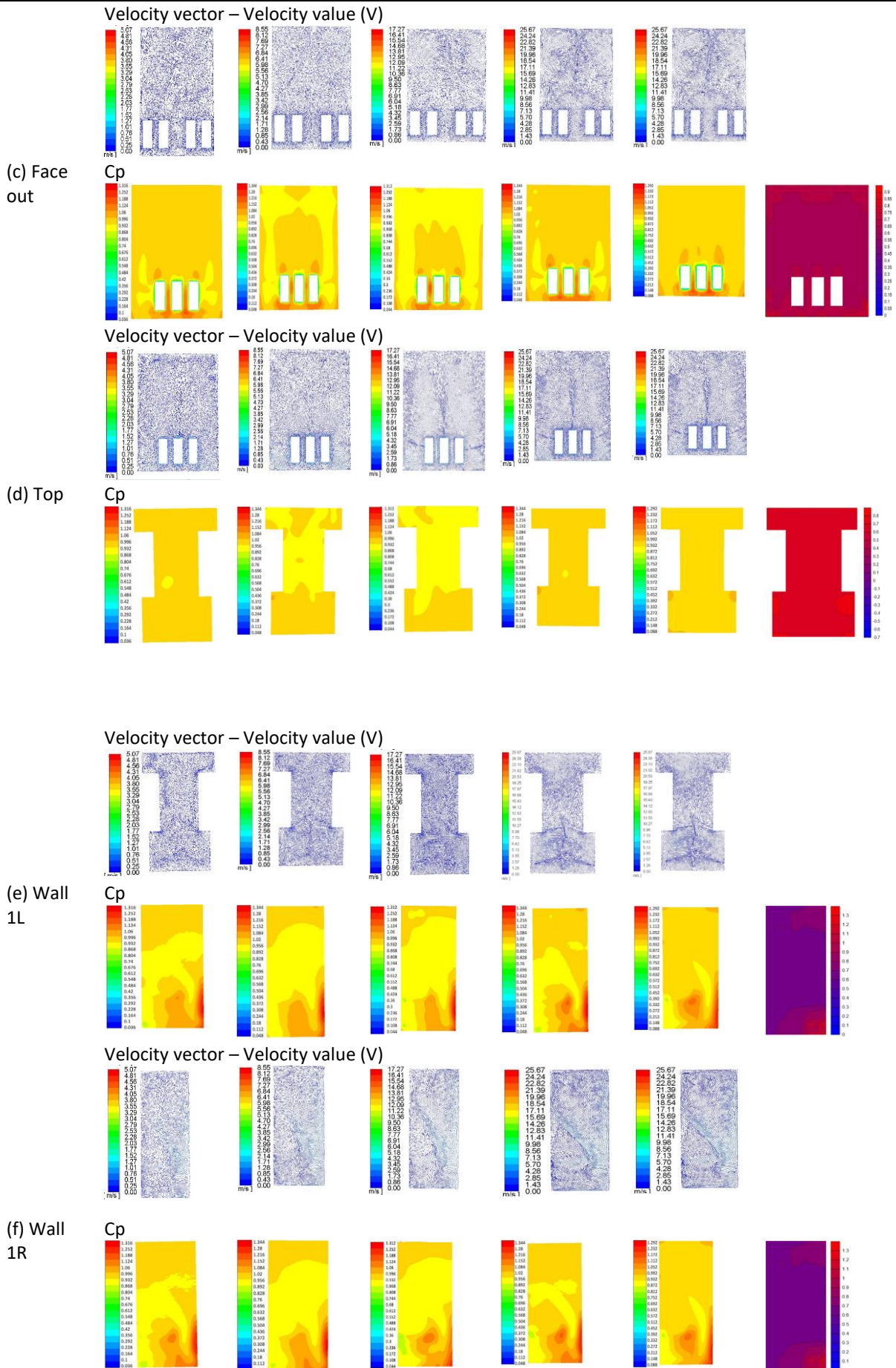
For the most part, it tends to be seen from these figures that the pressure increments at all edges of the model with a reduction occurring in the middle passage because of the reduction in the flow region. For both inlet and outlet walls, higher pressure values can be seen at the top segment contrasted with the lower partition because of the presence of window openings at this segment. Likewise, it can be seen that at the window openings, the pressure decreases significantly which can be credited to the small zone of the window openings. Moreover, it is commendable to take note of that uniform pressure conveyance is seen over the top wall (roof) of a model for both experimental and CFD results, which can be credited to the high elevation of the wall and the distance from the window openings.

Further, it can also be deduced, from the results of Table 3, that the velocity behaves on conversely to the pressure to such an extent that speed diminishes at all corners and at the wall intersections of the model with the expansion that happens in the center entry because of the reduction in the flow area. For both the inlet and outlet walls, lower values of the air speed can be seen at the top part contrasted with the lower portion because of the presence of the window openings at this segment. Additionally, it tends to be seen that at the window openings, the flow speed significantly increments because of the small area of the window openings. Furthermore, a uniform flow speed dissemination is noticed over the top wall (roof) of the model, which can be ascribed to the high rise of the wall and the good ways from the window openings.

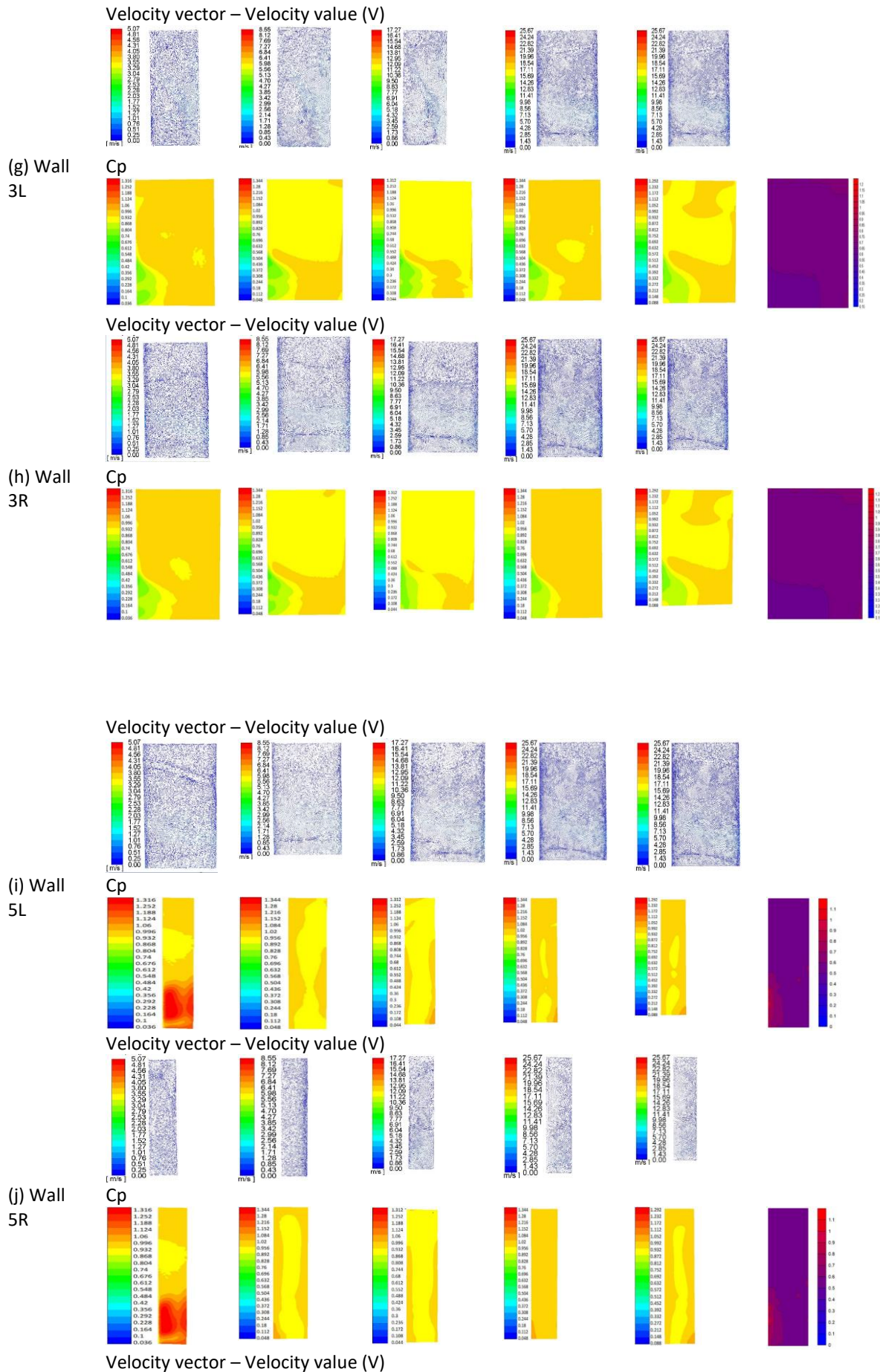
**Table 3**

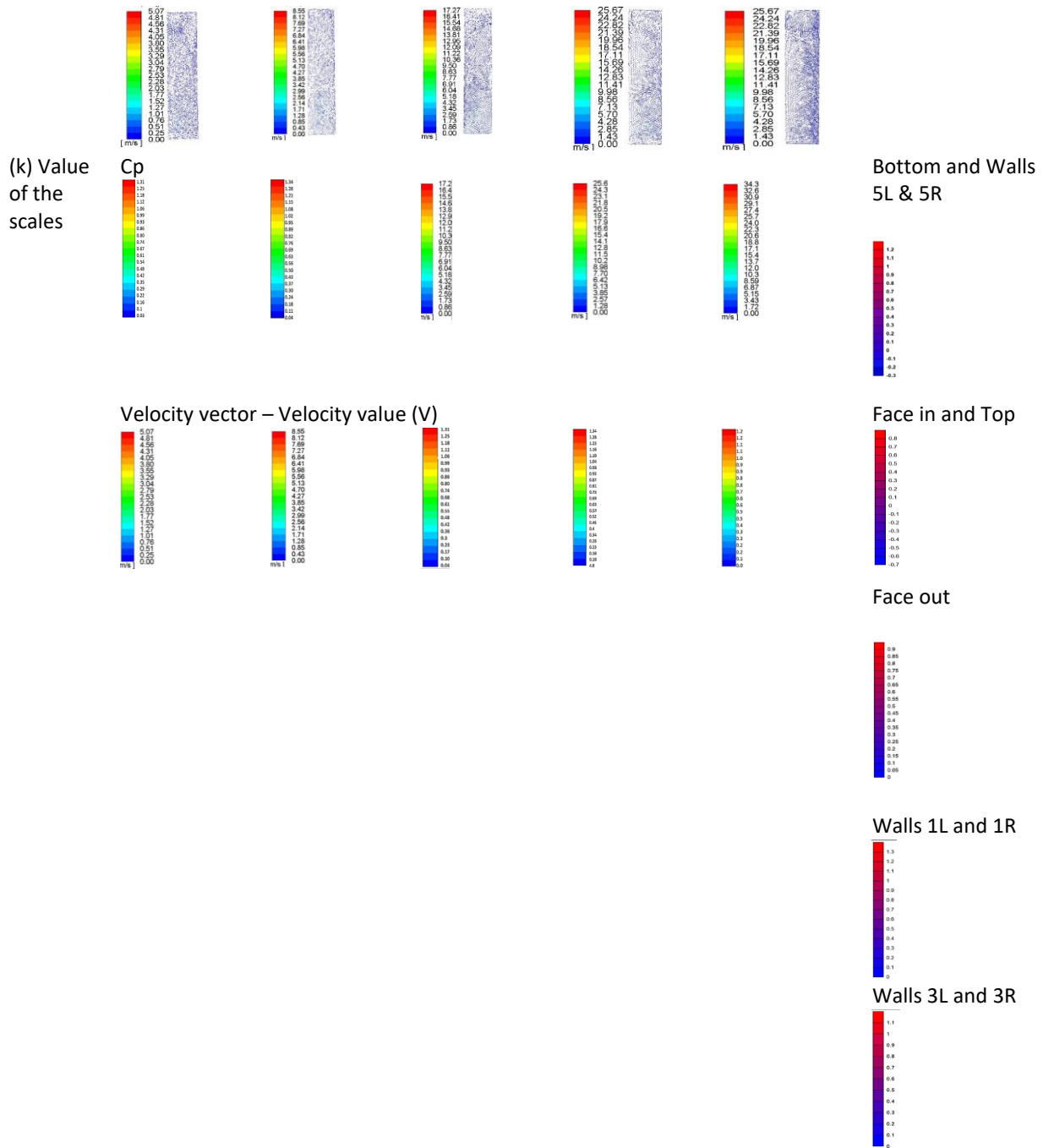
CFD and experimental results for the coefficient of pressure and the distributions velocity vectors at different flow levels for different inlet velocities

Face	CFD					Experimental V=20m/s
	V=3 m/s	V=5 m/s	V=10 m/s	V=15 m/s	V=20 m/s	
(a) Bottom	<b>Cp</b>					
						
(a) Bottom	<b>Velocity vector – Velocity value (V)</b>					
						
(b) Face in	<b>Cp</b>					
						





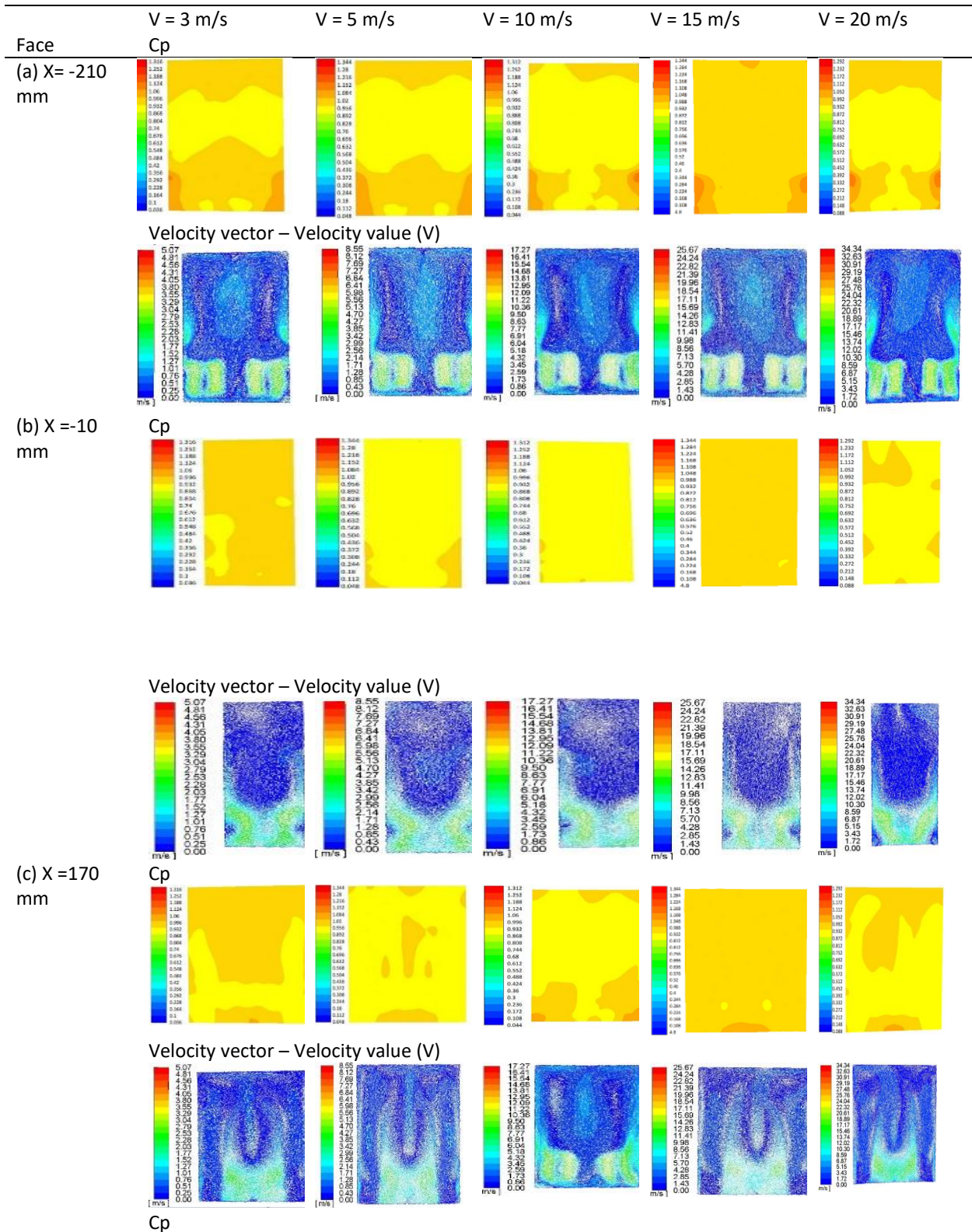




Cartesian directions; X, Y, and Z respectively. Table 4 demonstrate the contours for the three planes in the X-facilitate. These planes are perpendicular to the inlet airflow and distributed with distances of - 210 mm, 10 mm, and 170 mm, respectively, from the inlet face. By examining this table, an increase in air speed is seen at the entrance of the model joined by a decrease in pressure. At the inlet portion, the speed begins to diminish and the pressure increments. By moving through the intermediate passage, and because of the decrease in flow zone, the flow speed increments and the pressure diminishes. With the abrupt increment of an area that takes place at the exit portion, a speed decrease happens and appropriately an expansion in pressure happens. At the exit window openings, it can be noticed that the flow speed enormously increments with a decrease in pressure because of the adjustment in area because of the presence of window openings.

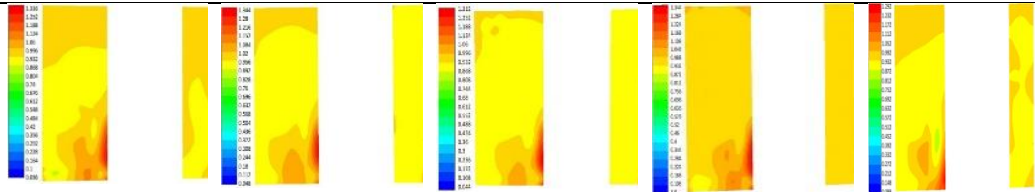
**Table 4**

CFD results for the coefficient of pressure and the distributions velocity vectors at different flow levels for different inlet velocities

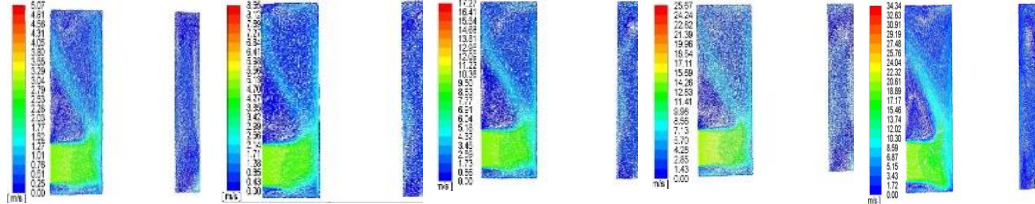




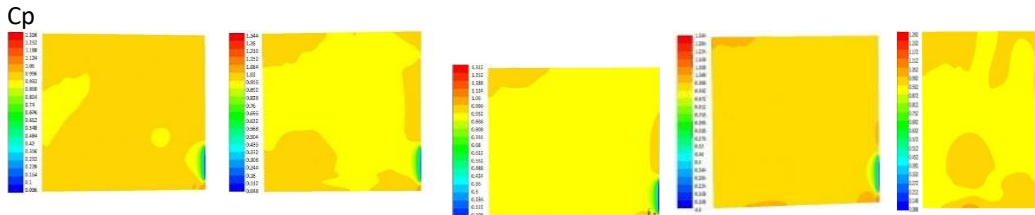
(d) Y = 110 mm



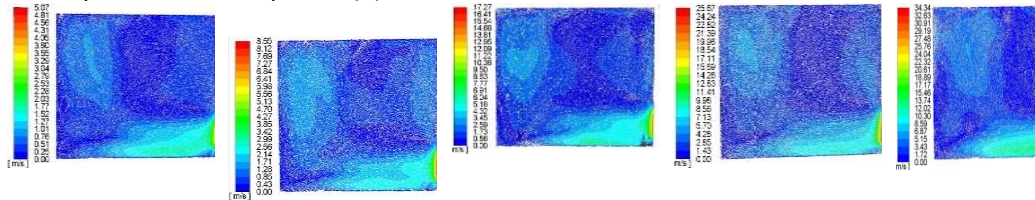
Velocity vector – Velocity value (V)



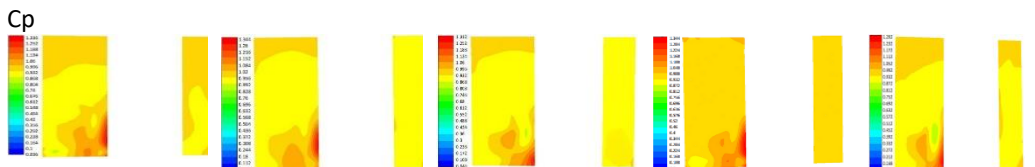
(e) Y = 0 mm



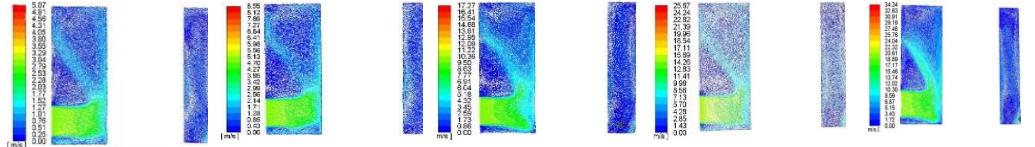
Velocity vector – Velocity value (V)



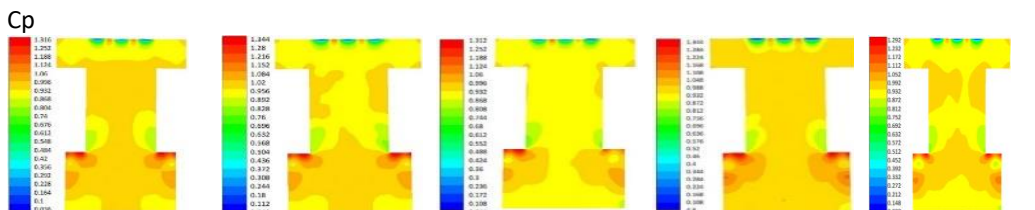
(f) Y = -110 mm



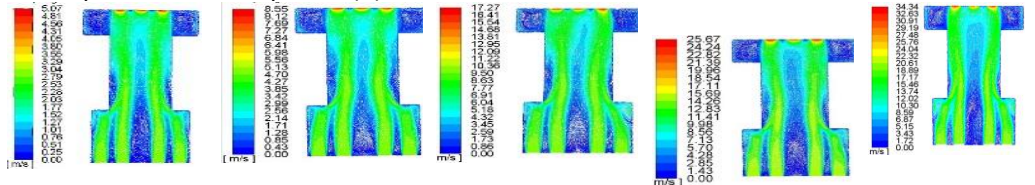
Velocity vector – Velocity value (V)



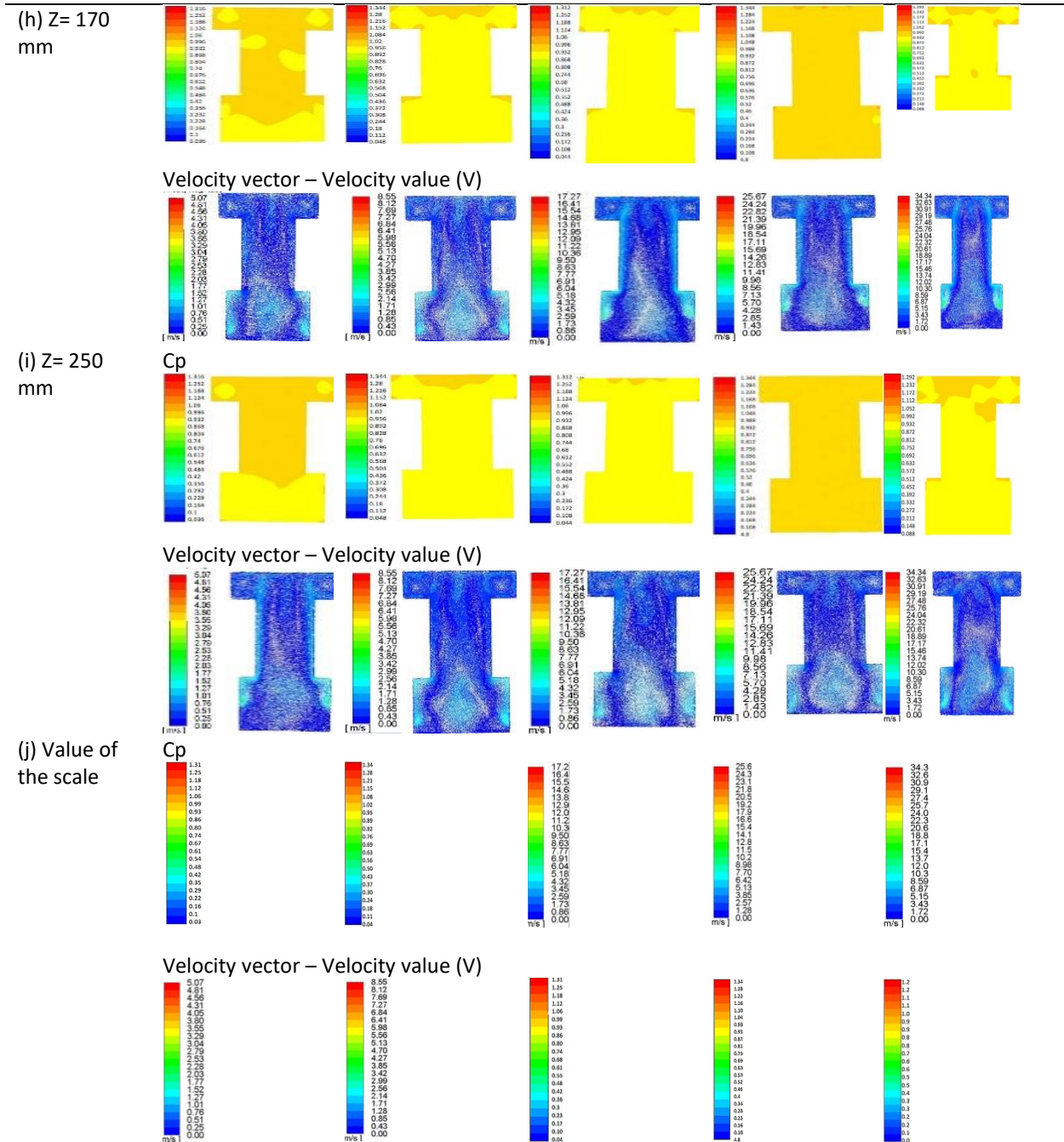
(g) Z = 70 mm



Velocity vector – Velocity value (V)



Cp



From the results of Table 4, CFD simulations anticipated the wind flow through the model from the inlet window openings and through the model, at that point at long last at the outlet from the other window openings. By analyzing this table, an increase of air speed is seen at the entrance of the model joined by a decrease in pressure. At the inlet portion, the speed begins to diminish and the pressure increments. By flowing through the middle of the intermediate passage, and because of the decrease in flow area, the flow speed increments and the pressure diminishes. With the sudden increase of area that happens at the exit portion, a speed decrease occurs and likewise, an expansion in the pressure takes place. At the exit window openings, it tends to be seen that the flow speed enormously increments with a decrease in pressure because of the adjustment in the area because of the presence of window openings.

In brief, the present study considered the natural ventilation of an ancient building in the historical area of Cairo, which is a Sultan Al-Ashraf Qaytbay mosque. Subsequently, the following important points can be stated:

- i. From Table 3 and Table 4, both represent the velocity of the air and  $C_p$  at the measuring/computational levels, the face to a distance of 1 m inside the model is one of the lowest places with a sense of the appropriate condition as the velocity change appears in the region at mid (A1).  $C_p$  is the highest limit on the corners (C1, C2), (C12, C11).
- ii. Area (A3) is better in terms of thermal comfort and air velocity as a result of the passage of air in a regular area without the presence of an obstacle except at (C10, C3) due to air turbulence as a result of its passing from area (A1), which is greater, to area (A2). As for area (A3), it is found that the best places are the space between (C4, C9) and the lowest at corners (C4, C5, C6, C7, C8, C9) due to the change in area from (A2) to (A3), also, at the exit windows (W5), W6, W7).
- iii. Feeling of a bad breath is expected due to the exit of hot air after passing in (A1, A2) at the level of the worshipers while sitting, as the Islamic rites require that the worshipers sit until the rituals are erected on the ground, which is approximately 0.8 m above the floor of the mosque.
- iv. In order to improve the situation inside the mosque for a better feeling of comfort, the closed windows above the front and back windows (W1: W4) (W5: W7) and the air traps/catchers in the mosque in area (A2) at the corners (C3, C4, C9, C10) should be reopened. It is better for places with weak air influence.

## 5. Conclusions

Based on the present study and the above results and discussions, the following points can be also enlisted.

- i. The architecture design of the mosque is appropriate for the time of its construction.
- ii. Currently and because of the presence of buildings/structures encompassing the mosque, a decrease in the amount and nature of wind current inside the mosque is seen, which prompts a decrease in wind flow inside the mosque by obstructing the windows. Accordingly, a reduction of thermal comfort is expected due to the increase in the air temperature.
- iii. The air traps/catchers in the mosque in area (A2) at the corners (C3, C4, C9, C10) should be reopened. It is better for places with weak air influence.
- iv. The present examination proposes that this ancient architecture design of the mosque ought to be modified to improve the air distribution through the mosque and enhance the mosque ventilating efficacy under the present situation.

## References

- [1] Baker, Nick, and Koen Steemers. *Energy and environment in architecture: a technical design guide*. Taylor & Francis (1<sup>st</sup> Ed.), 2003.  
<https://doi.org/10.4324/9780203223017>
- [2] Haynes, Oscar T. *Natural Ventilation: Strategies, Health Implications and Impacts on the Environment*. Nova Science Pub Inc, 2015.
- [3] Williams, Caroline. *Islamic monuments in Cairo: the practical guide*. American Univ in Cairo Press, 2008.
- [4] Allocca, Camille, Qingyan Chen, and Leon R. Glicksman. "Design analysis of single-sided natural ventilation." *Energy and Buildings* 35, no. 8 (2003): 785-795.  
[https://doi.org/10.1016/S0378-7788\(02\)00239-6](https://doi.org/10.1016/S0378-7788(02)00239-6)
- [5] Song, Jiafang, and Xiangquan Meng. "The improvement of ventilation design in school buildings using CFD simulation." *Procedia Engineering* 121 (2015): 1475-1481.



- <https://doi.org/10.1016/j.proeng.2015.09.073>
- [6] Wang, Jihong, Tengfei Zhang, Shugang Wang, and Francine Battaglia. "Numerical investigation of single-sided natural ventilation driven by buoyancy and wind through variable window configurations." *Energy and Buildings* 168 (2018): 147-164.  
<https://doi.org/10.1016/j.enbuild.2018.03.015>
- [7] Deng, Xiang, and Zijing Tan. "Numerical analysis of local thermal comfort in a plan office under natural ventilation." *Indoor and Built Environment* (2019): 1-15.  
<https://doi.org/10.1177/1420326X19866497>
- [8] Wu, Yu-Chou, An-Shik Yang, Li-Yu Tseng, and Chin-Lung Liu. "Myth of ecological architecture designs: Comparison between design concept and computational analysis results of natural-ventilation for Tjibaou Cultural Center in New Caledonia." *Energy and Buildings* 43, no. 10 (2011): 2788-2797.  
<https://doi.org/10.1016/j.enbuild.2011.06.035>
- [9] Stavrakakis, G. M., P. L. Zervas, H. Sarimveis, and N. C. Markatos. "Optimization of window-openings design for thermal comfort in naturally ventilated buildings." *Applied Mathematical Modelling* 36, no. 1 (2012): 193-211.  
<https://doi.org/10.1016/j.apm.2011.05.052>
- [10] Mohamed, Mohd Farid, Steve King, Masud Behnia, and Deo Prasad. "The effects of balconies on the natural ventilation performance of cross-ventilated high-rise buildings." *Journal of Green Building* 9, no. 2 (2014): 145-160.  
<https://doi.org/10.3992/1943-4618-9.2.145>
- [11] von Grabe, Jörn, Petr Svoboda, and Armin Bäumlner. "Window ventilation efficiency in the case of buoyancy ventilation." *Energy and Buildings* 72 (2014): 203-211.  
<https://doi.org/10.1016/j.enbuild.2013.10.006>
- [12] Elshafei, Ghada, Abdelazim Negm, Mahmoud Bady, Masaaki Suzuki, and Mona G. Ibrahim. "Numerical and experimental investigations of the impacts of window parameters on indoor natural ventilation in a residential building." *Energy and Buildings* 141 (2017): 321-332.  
<https://doi.org/10.1016/j.enbuild.2017.02.055>
- [13] Zhou, Junli, Cheng Ye, Yan Hu, Hassan Hemida, Guoqiang Zhang, and Wei Yang. "Development of a model for single-sided, wind-driven natural ventilation in buildings." *Building Services Engineering Research and Technology* 38, no. 4 (2017): 381-399.  
<https://doi.org/10.1177/0143624417699658>
- [14] Heracleous, C., and A. Michael. "Experimental assessment of the impact of natural ventilation on indoor air quality and thermal comfort conditions of educational buildings in the Eastern Mediterranean region during the heating period." *Journal of Building Engineering* 26 (2019): 100917.  
<https://doi.org/10.1016/j.jobe.2019.100917>
- [15] Wong, Nyuk Hien, and Sani Heryanto. "The study of active stack effect to enhance natural ventilation using wind tunnel and computational fluid dynamics (CFD) simulations." *Energy and Buildings* 36, no. 7 (2004): 668-678.  
<https://doi.org/10.1016/j.enbuild.2004.01.013>
- [16] Chu, Chia-Ren, Y-H. Chiu, Yi-Ting Tsai, and Si-Lei Wu. "Wind-driven natural ventilation for buildings with two openings on the same external wall." *Energy and Buildings* 108 (2015): 365-372.  
<https://doi.org/10.1016/j.enbuild.2015.09.041>
- [17] Wang, Haojie, Panagiota Karava, and Qingyan Chen. "Development of simple semiempirical models for calculating airflow through hopper, awning, and casement windows for single-sided natural ventilation." *Energy and Buildings* 96 (2015): 373-384.  
<https://doi.org/10.1016/j.enbuild.2015.03.041>
- [18] Sacht, Helenice, Luis Bragança, Manuela Almeida, and Rosana Caram. "Study of natural ventilation in wind tunnels and influence of the position of ventilation modules and types of grids on a modular façade system." *Energy Procedia* 96 (2016): 953-964.  
<https://doi.org/10.1016/j.egypro.2016.09.173>
- [19] Noman, Fawaz Ghaleb, Nazri Kamsah, and Haslinda Mohamed Kamar. "Improvement of thermal comfort inside a mosque building." *Jurnal Teknologi* 78, no. 8-5 (2016): 9-18.  
<https://doi.org/10.11113/jt.v78.9579>
- [20] Bughrara, Khaled SM, Zeynep Durmuş Arsan, and Gül den Gökçen Akkurt. "Applying underfloor heating system for improvement of thermal comfort in historic mosques: the case study of Salepçioğlu Mosque, Izmir, Turkey." *Energy Procedia* 133 (2017): 290-299.  
<https://doi.org/10.1016/j.egypro.2017.09.390>
- [21] Hussin, Azman, Lim Chin Haw, Sohif Mat, Ahmad Fazlizan, and Elias Salleh. "Indoor Thermal Performance of a Retrofitted Air-Conditioned Mosque: Case Study for Penang State Mosque." *Jurnal Kejuruteraan* 1, no. 3 (2018): 37-45.

- [https://doi.org/10.17576/jkukm-2018-si1\(3\)-06](https://doi.org/10.17576/jkukm-2018-si1(3)-06)
- [22] Atmaca, A. B., and G. Zorer Gedik. "Evaluation of mosques in terms of thermal comfort and energy consumption in a temperate-humid climate." *Energy and Buildings* 195 (2019): 195-204.  
<https://doi.org/10.1016/j.enbuild.2019.04.044>
- [23] Egyptian Ministry of Antiquities. Accessed March 24, 2020.  
<http://www.antiquities.gov.eg/DefaultAr/Pages/default.aspx>.
- [24] Cui, Can, Wenjian Cai, and Haoran Chen. "Airflow measurements using averaging Pitot tube under restricted conditions." *Building and Environment* 139 (2018): 17-26.  
<https://doi.org/10.1016/j.buildenv.2018.05.014>
- [25] Keramidas, George A., and C. A. Brebbia. *Computational methods and experimental measurements: proceedings of the international conference, Washington, D.C. July 1982*. Springer-Verlag, 1982.  
<https://doi.org/10.1007/978-3-662-11353-0>
- [26] ANSYS, Inc. "Ansys Fluent." Ansys. 2020. <https://www.ansys.com/products/fluids/ansys-fluent>.
- [27] ANSYS DesignModeler. "Introduction to Ansys DesignModeler." Ansys. 2020.  
<https://www.ansys.com/services/training-center/platform/introduction-to-ansys-designmodeler>